Too fat or not too fat? – This is the question

e-Poster: EE-087

Congress: ESGAR 2014

Type: Educational Exhibit

Topic: Diagnostic / Liver - Other

Authors: C. Oliveira, I. Candelária, R. Catarino, L. Curvo-Semedo, F. Caseiro-Alves; Coimbra/PT

1. Learning Objectives

To review the typical and atypical imaging findings of focal fatty infiltration (FFI) and focal fatty sparing (FFS) in the liver.

To focus on their distribution pattern, differential diagnosis and pathophysiological mechanisms.

To discuss the non-invasive role of imaging for the diagnosis and the impact on patient management.

2. Background

Fat changes - typical patterns

Liver steatosis is a common finding on cross-sectional imaging studies. Different patterns of hepatic steatosis and focal fat sparing distribution are described in the literature (Table 1).

Table 1

	Pattern distribution
Steatosis	Diffuse Focal - Nodular - Subcapsular - Perivascular - Perilesional Multinodular
Fat sparing	Focal - Nodular - Subcapsular - Perivascular - Perilesional

Table 1 - Pattern distribution types of steatosis and fat sparing in the liver.

Diffuse hepatic steatosis

Diffuse hepatic steatosis is the most common distribution pattern. It results from an abnormal lipid accumulation in the hepatocytes and is associated with an inflammatory process and potential progression to fibrosis.

One of the commonest causes is alcohol abuse (which interferes with mitochondrial function). Diabetes mellitus, obesity, exogenous steroids, drugs (amiodarone, methotrexate, chemotherapy) and

IV hyperalimentation are also related to diffuse steatosis infiltration. This so well-known nonalcoholic fatty liver disease is being recognized as a disease associated to liver-related morbidity and even mortality. Its prevalence has been rising in the past two decades to become the leading cause of chronic liver disease.

When there is a diffuse pattern usually the diagnosis is quite straightforward. Focal fatty infiltration (FFI) and focal fatty sparing (FFS) are conditions that more frequently can pose potential diagnostic dilemmas and consequently affect patient management.

Focal fatty changes

FFI is less common than diffuse hepatic fat infiltration. Vascular disturbances are in the pathogenesis of these hepatic FFI changes due to reduced portal flow and increased insulin entry (inducing triglycerides esterification). This feature was first described in patients with intraperitoneal insulin administration that had a peculiar subcapsular pattern of hepatic steatosis distribution.
Third inflow pathways are one of the causes of vascular disturbances, due to the relative decrease in portal flow.

Characteristic locations for focal fatty changes are related to the typical areas of these vascular disturbances. They include the medial segment of the left lobe of the liver (segment IV) either anterior to the porta hepatis or adjacent to the falciform ligament, the gallbladder fossa and subcapsular areas (Table 2, Figures 1 and 2).

Table 2

Location	Abnormal venous flow
Medial portion of segment IV	Gastric or pancreaticoduodenal veins
Adjacent to the *porta hepatis*	Parabiliary venous system
Adjacent to the falciform ligament	Sappey veins
Gallbladder fossa	Paracolecystic venous system
Subcapsular parenchyma	Subfrenic veins

Table 2 - Typical locations of focal fat changes in hepatic parenchyma.

Figure 1

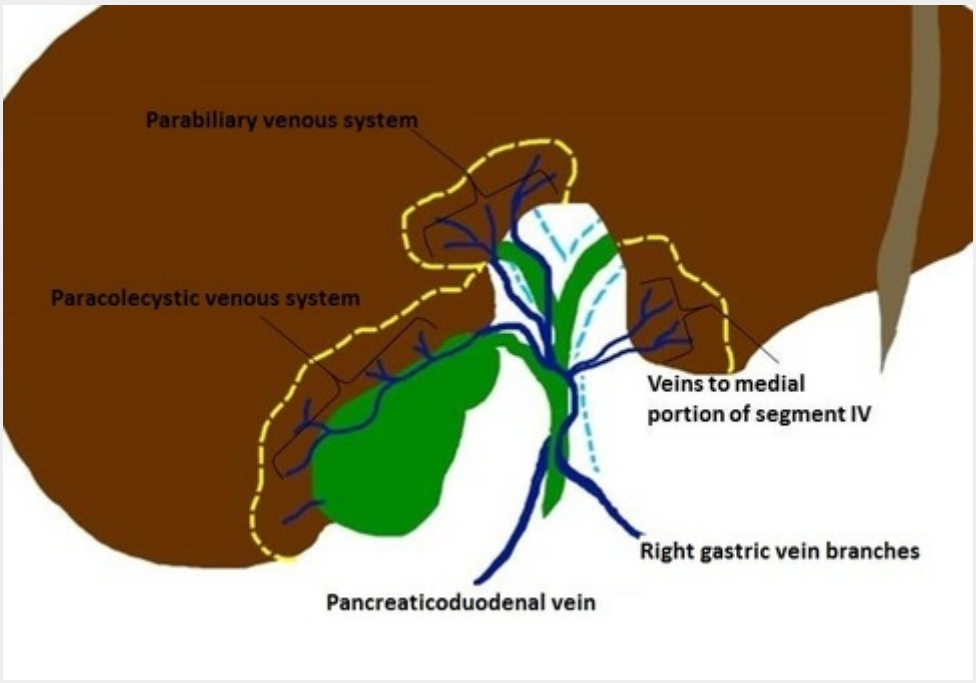

Figure 1 - Schematic draw showing parabiliary and paracolecystic venous system and branches from pancreaticoduodenal and right gastric veins responsible for anomalous venous flow in characteristic parenchymal areas.

Figure 2

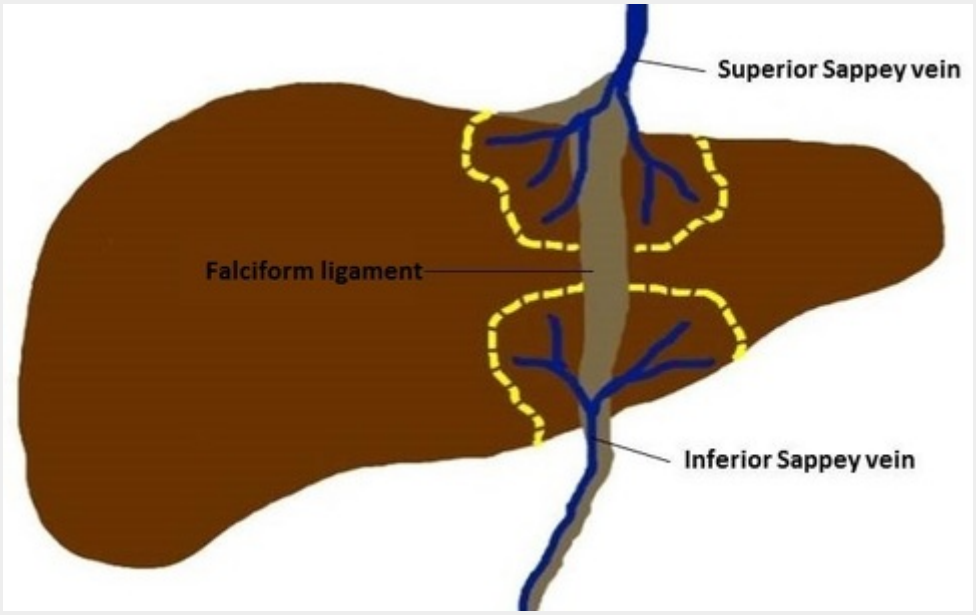

Figure 2 - Schematic draw showing superior and inferior Sappey veins responsible for anomalous venous flow near the falciform ligament.

In focal fat sparing (FFS), the typical locations are the same as the ones described for FFI, as they also

are related to changes in vascular supply (in this case due to by-pass on nutrients entry).

These vascular changes can also occur nearby some hepatic lesions, especially the hypervascular ones, leading to perilesional focal fat changes.

Intralesional fat

Some primary liver neoplasms (e.g. hepatocellular adenoma, well-differentiated HCC and rare cases of FNH) can be more or less lipid-rich contributing to increase the diagnostic uncertainty.

Imaging techniques in fatty changes evaluation

Ultrasound

Ultrasound (US) is usually the first imaging modality to evaluate liver fat infiltration. US features become apparent when the amount of fat reaches 15-20%. The basic ultrasound feature is the increased beam reflectivity, leading to increased parenchyma echogenicity. Focal fat sparing areas appear hypoechoic relative to the surrounding parenchymal.

Contrast enhanced ultrasound study can be helpful in diagnose focal fat changes as they have the same enhancement pattern as the rest of the liver parenchyma.

CT

In CT, normal liver has attenuation values between 50-60 HU. Fat infiltration leads to a decrease by 1.6 HU per mg of fat in each gram of liver. A simplest way is to compare liver and spleen attenuation, usually a difference greater than 10 UH on unenhanced images is found in steatosis. There is also a decreased attenuation on post contrast CT. Liver and spleen should normally be similar on delayed (70 second) scans, but the earlier scans are unreliable as the spleen enhances earlier than the liver (systemic supply rather than portal).

MR

Liver MR is currently the state-of-the-art imaging tool for the accurate non-invasive characterization of fat infiltration, especially of the pseudo-nodular forms of FFS or FFI. Two main techniques are used to detect fat: chemical shift and fat saturation sequences.

Chemical shift is useful to identify the presence of microscopic fat (hepatic steatosis, adenomas). Protons (H+) in water molecules have a slightly higher resonance frequency than in lipids. So, in a 1,5T magnetic field, protons in water and lipids are out-of-phase in TE: 2,3ms and in-phase in TE: 4,6ms. When out of phase, the signal is canceled out and drops off. Always remind that if iron is present, this will affect the magnetic field so this technique should not be applied.

Fat saturation techniques are used to identify macroscopic fat. First, a fat selective saturation pulse is applied to cancel the magnetization of the lipids, so the fat signal will be null. Then the excitation pulse is sent, but as the lipids have no signal, no magnetization will be tilted. It's a fat selective sequence, but more time consuming and more prone to susceptibility artifacts.

Quantitative methods

Some non-invasive imaging methods, such as magnetic resonance spectroscopy (MRS) and multiecho (more than 6 echos) gradient-echo imaging with or without fat spectral modeling have been used to accurately quantify liver fat. Fat fraction mapping (FFM) has also recently revealed to be an option in fat quantification (Figure 3).

Figure 3

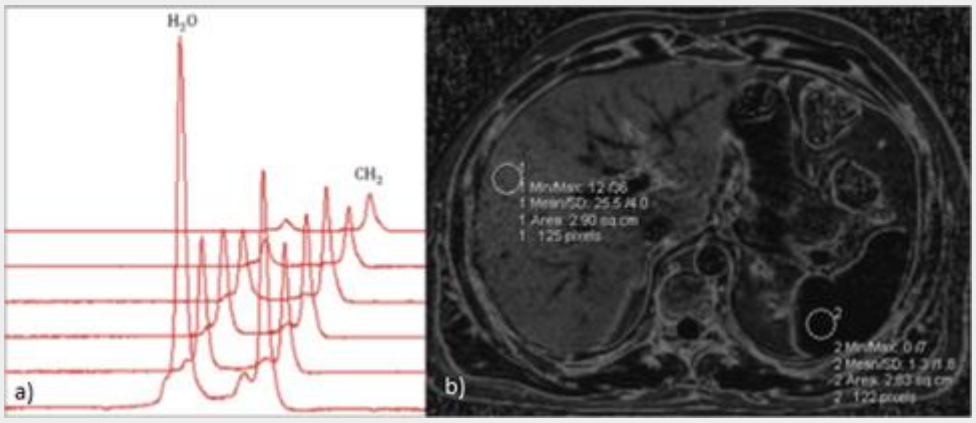

Figure 3 - Patient with hepatic steatosis. MRS analyses (a) and fat fraction mapping analyse (b) in a fat quantification study.

3. Imaging Findings/Procedure Details

Diffuse hepatic steatosis

In ultrasound images, diffuse hepatic steatosis appears as an increased hepatic echogenicity and inability to visualize the portal vein walls, as the parenchyma becomes brighter. A comparison with the right kidney echogenicity can be made: in normal liver they have nearly the same echogenicity (Figure 4).

Figure 4

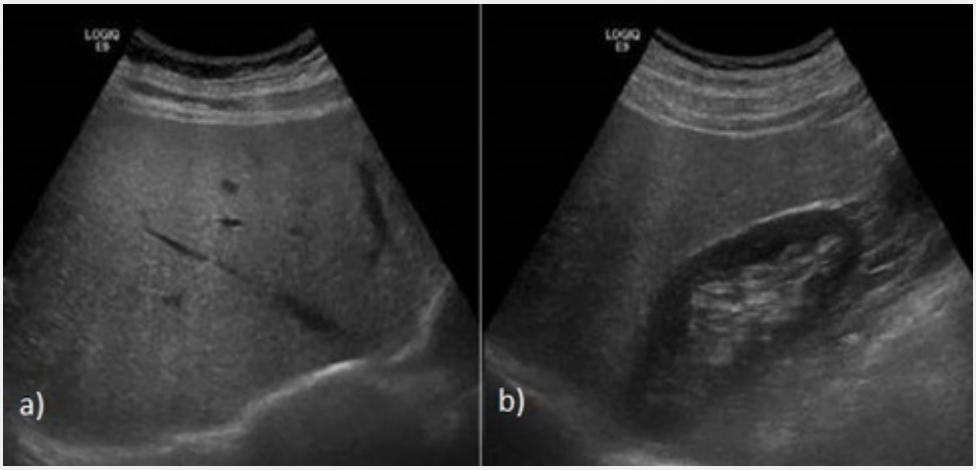

Figure 4 - Ultrasound images in a patient with diffuse hepatic steatosis showing increased hepatic parenchyma echogenicity (a). Note the reflectivity differences between the liver and the right kidney (b).

Figure 5

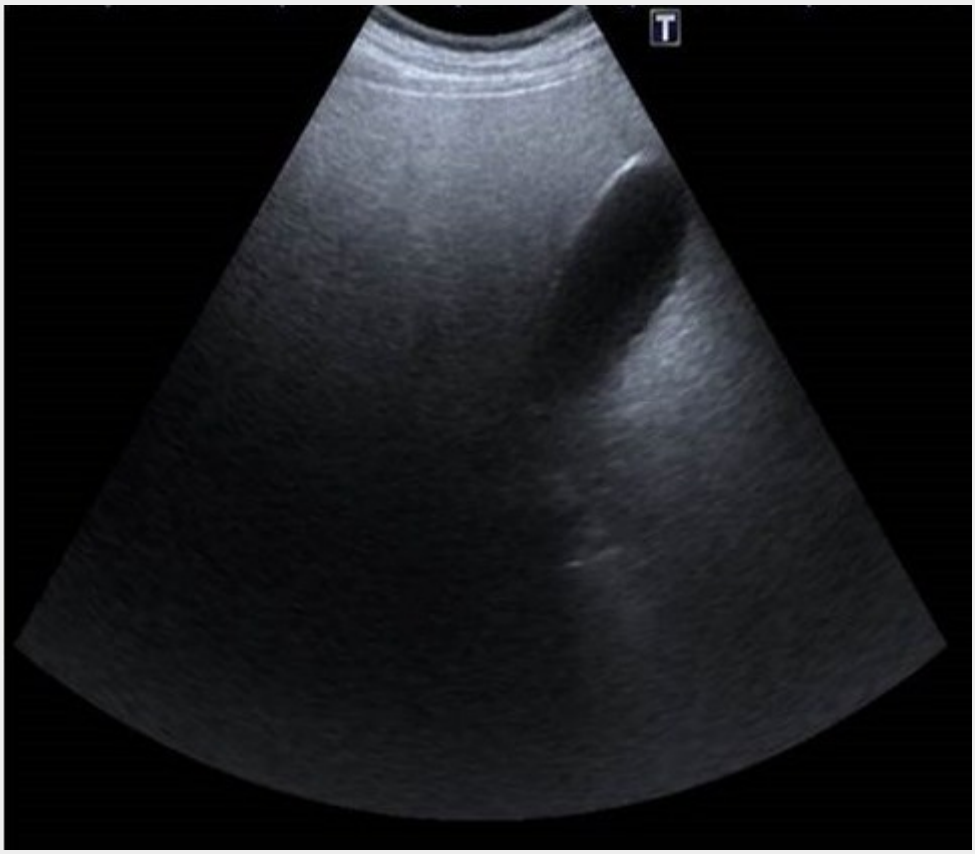

Figure 5 - Ultrasound image in a severe case of hepatic steatosis. There is a very high attenuation of the ultrasound beam caused by the diffuse fat infiltration.

In severe cases the attenuation of the beam is so high that deep areas become very difficult to visualize (Figure 5).

In CT, as described before, there is a decrease in the liver parenchyma attenuation. In severe cases, an inverted vascular pattern may be found, with hyperdense vessels compared to low attenuation parenchyma (Figure 6).

Figure 6

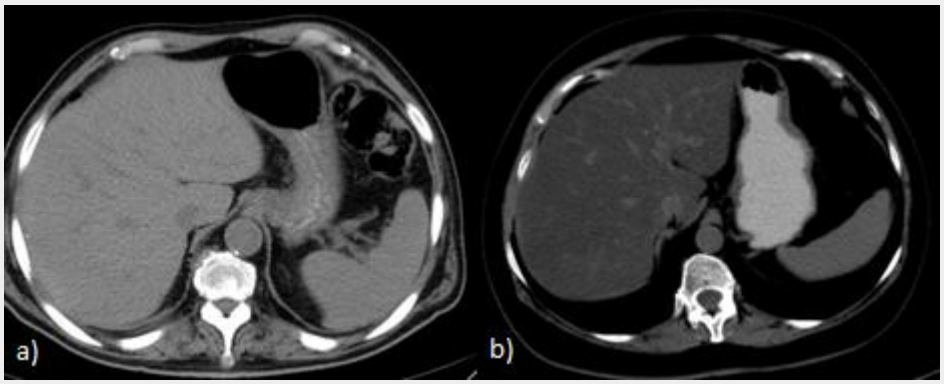

Figure 6 - CT non-contrast axial images showing normal hepatic parenchyma density (a) and a severe case of diffuse fat infiltration with a reversed vascular pattern (b).

MRI emplying in and out-of-phase T1-w images is the most accurate method to identify diffuse fat infiltration. The presence of a diffuse drop-off in the signal intensity (SI) in out-of-phase sequence confirms the presence of microscopic fat (Figure 7).

Figure 7

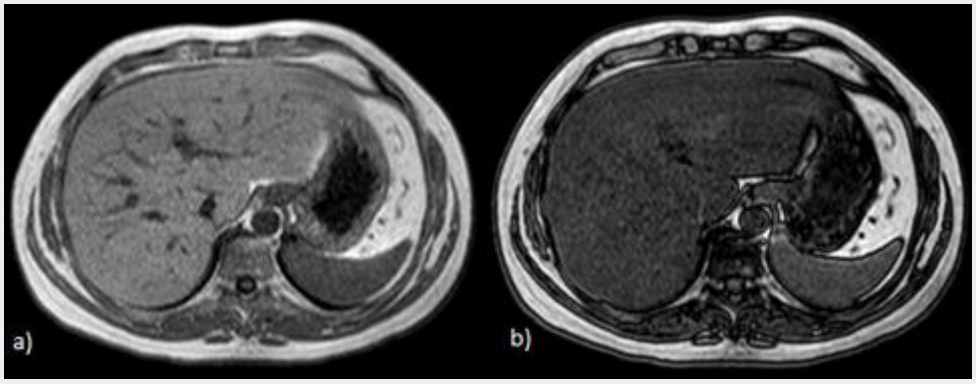

Figure 7 - MR T1-w in-phase (a) and out-of-phase imaging (b). Note the diffuse drop-off of SI in out-of-phase imaging (b) due to the presence of microscopic fat.

An important clinical feature in diffuse fat infiltration is not only bland steatosis infiltration, but also steatohepatitis, which can progress to fibrosis, cirrhosis, and ultimately hepatocellular carcinoma (Figure 8).

Figure 8

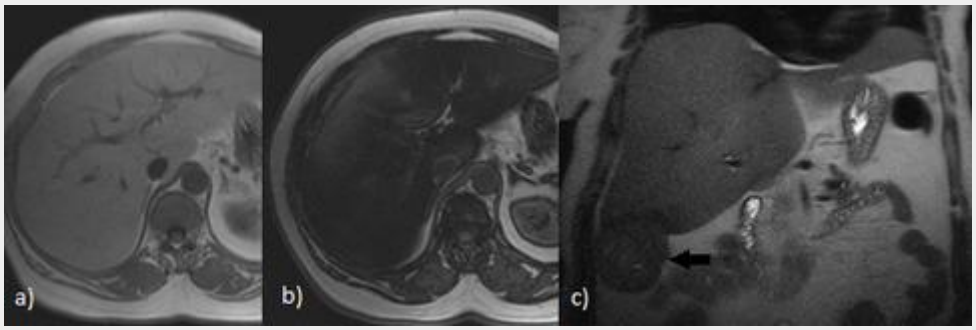

Figure 8 - MR T1-w in-phase (a) and out-of-phase imaging (b) showing diffuse hepatic steatosis. (c) MR T2-w imaging in the coronal plane of the same patient revealing a nodular lesion (black arrow): a hepatocellular carcinoma diagnosis was made.

Focal fat infiltration

Nodular FFI

Nodular focal fat changes are a frequent cause of diagnostic dilemma. Basic imaging features of focal of fat changes, included not only the typical location (Table 2 - in Background section), but also geographical well defined margins, with no mass effect nor vessels distortions (Figures 9 to 11).

Figure 9

Figure 9 - Ultrasound image showing a nodular periportal hyperechogenic lesion in a midle-age female patient.

Figure 10

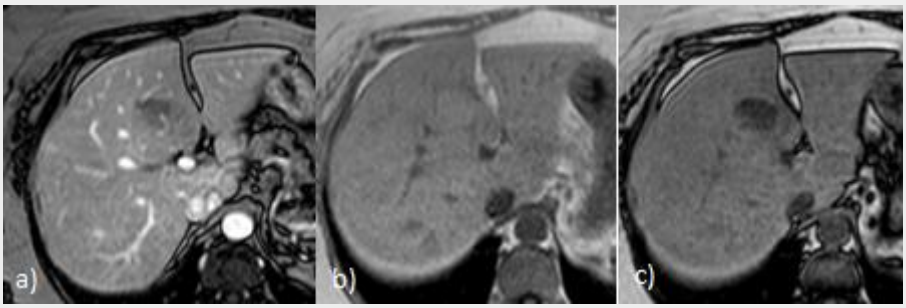

Figure 10 - Same patient in Figure 9. MR axial T1-w imaging after gadolinium injection (a) no vessel distortion is noted. In T1-w in-phase (b) and out-of-phase (c) imaging there is a diffuse SI drop-off in out-of-phase sequence confirming that the nodular area corresponds to a focal fat infiltration area.

Figure 11

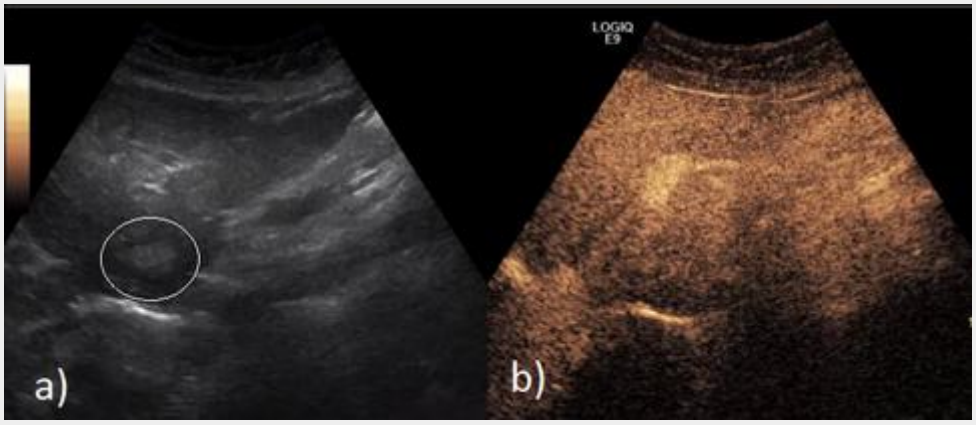

Figure 11 - Contrast enhanced US may help to identified focal fat infiltration areas. In steatotic areas, enhancement equals the rest of the liver parenchyma (b); fat infiltration area is only identified in B-mode images (a).

Segmental fat infiltration

Sometimes the aberrant vessel causing the focal fat change can be identified (Figure 12).

Figure 12

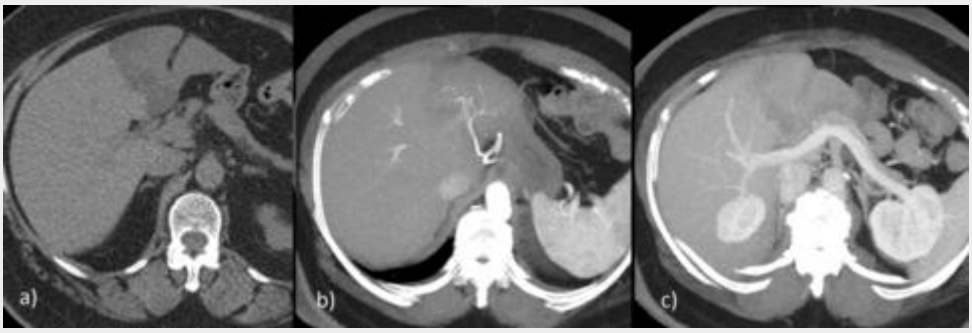

Figure 12 - CT axial image (a) and MIP reconstructions (b and c) showing a segmental fat infiltration distribution. In non-enhanced image there is diffuse low attenuation in the left lobe (a), post contrast in late arterial (b) and portal phase (c) reveal an increase in arterial flow by left gastric artery branches (b) and no left portal venous flow (c).

Perilesional fat infiltration

Perilesional fat infiltration can occur due to changes in the vascular flow or due to local effects of metabolic products. In insulinoma metastases for example, the peripheral steatotic pattern seen is due to local insulin effect.

Subcapsular fat infiltration

Fatty changes localised to the subcapsular region are a rare (Figure 13), usually occurring in individuals receiving continuous ambulatory peritoneal dialysis with intraperitoneal insulin therapy.

Figure 13

Figure 13 - Subcapsular steatosis. Non-enhanced CT images (a to c) in a patient with a subcapsular distribution of fat infiltration (lower attenuation areas).

Perivascular fat infiltration

It's an atypical manifestation of focal fat infiltration affecting areas around portal and hepatic veins.

Multinodular fat infiltration

Some atypical manifestations of fat infiltration have a diffuse multinodular pattern that may be difficult to diagnose. In these cases MRI imaging or biopsy may be necessary. Main differential diagnosis is adenomatosis, in which a hypervascular enhancement of the nodules is seen, but not in multinodular steatosis (Figure 14).

Figure 14

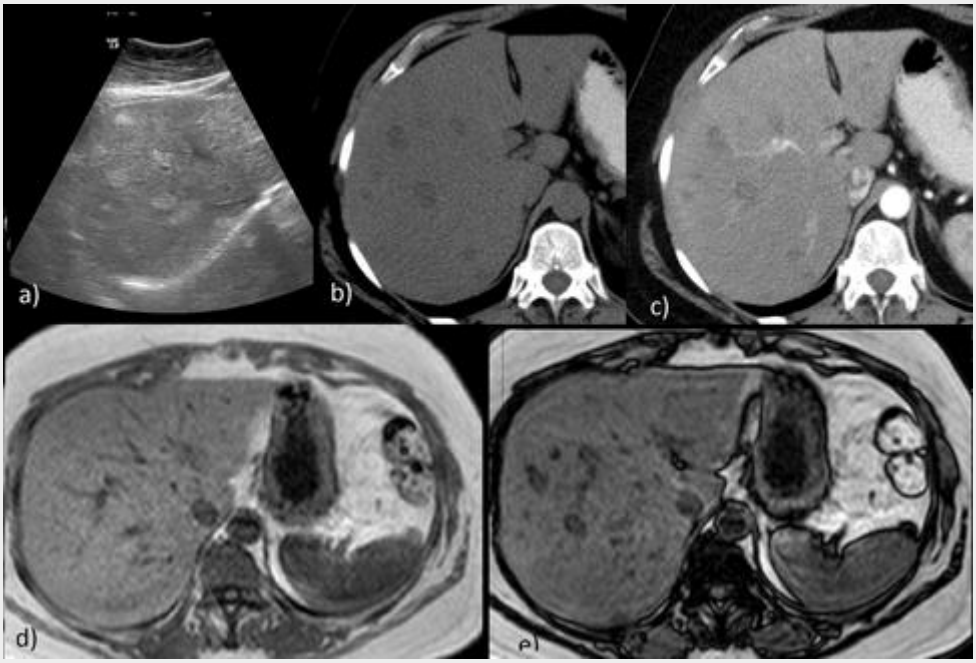

Figure 14 - Multinodular steatosis. Ultrasound (a) shows hyper echogenic nodular lesions; in CT axial non-enhanced images there are several hypo attenuated lesions that don't enhance after contrast (b and c). In MRI T1-w out-of-phase imaging there is SI drop-off of the nodular lesions (e).

Focal fat sparing

Focal fat sparing (FFS) also occurs in characteristic locations (Table 2 - in Background) and often has geographic margins such as in the FFI. Similarly, there is neither mass effect nor vessels distortion. Atypical locations can be mistaken for tumoral lesions specially if presenting with a nodular morphology. In these difficult cases, MR imaging is used to identified the microscopic fat infiltration of the remaining liver parenchyma. Biopsy may be required in some cases.

Nodular fat sparing

The most typical location of FFS is the postero medial portion of IV segment (Figures 15 to17). Typical location and morphology are two important imaging features of FFS.

Figure 15

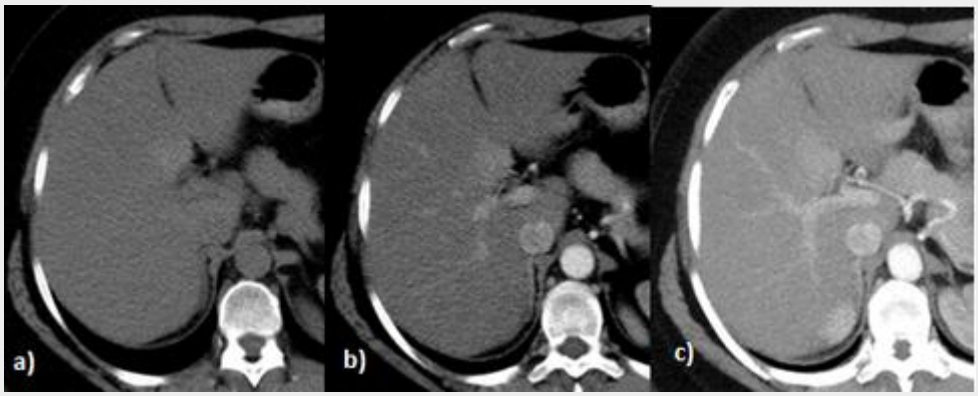

Figure 15 - Focal fat sparing in the postero medial portion of IV hepatic segment. There is a discrete higher attenuation in non-enhanced image (a). After contrast we can see that there is no vascular distortion (a vessel runs through it) and the geographical margins are better defined (b and c).

Figure 16

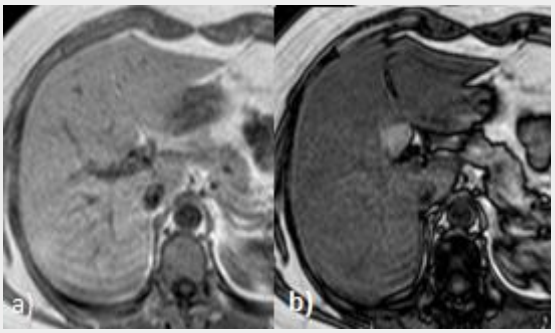

Figure 16 - Same patient in Figure 13. In MR T1-w out-of-phase imaging (b) there is a diffuse drop-out of SI, except in the posterior medial aspect of the IV segment - focal fat sparing.

Figure 17

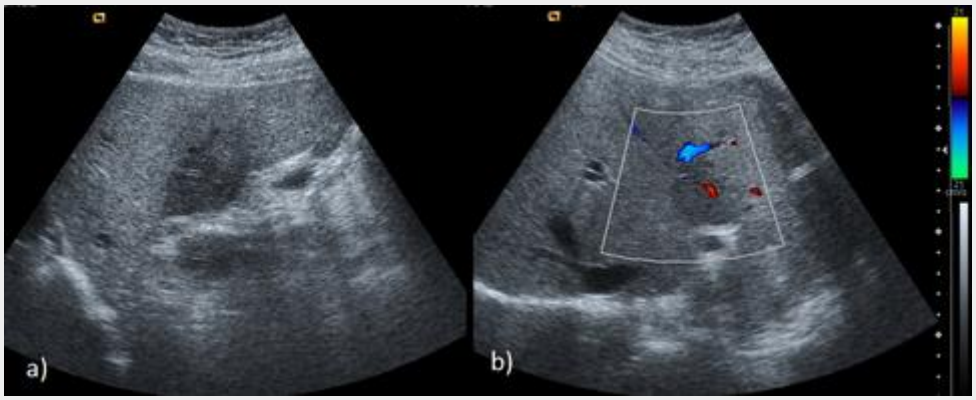

Figure 17 - Ultrasound images showing a hypoechoic area in the left lobe (a); no vessel distortion is shown in Doppler study (b); these are characteristic features of FFS area. No enhancing lesion was found in CT study (not shown).

The gallbladder fossa and periportal areas are two other very frequent areas of FFS (Figures 18 and 19).

Figure 18

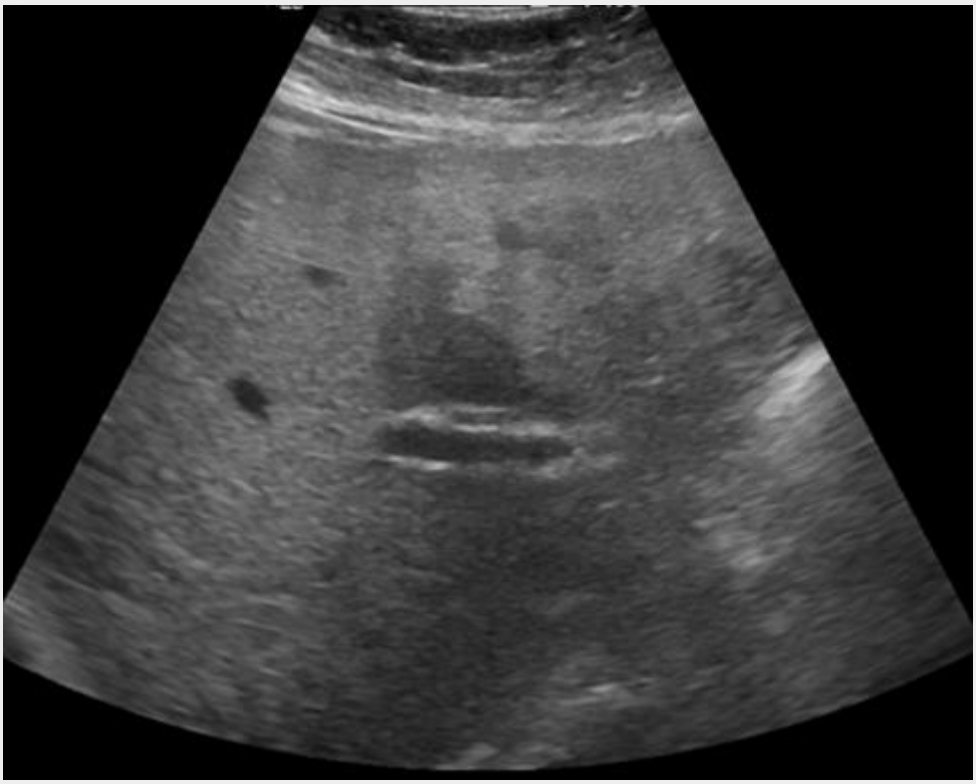

Figure 18 - Typical periportal location of FFS. Note the geographical margins and no mass-effect of the hypoechoic area.

Figure 19

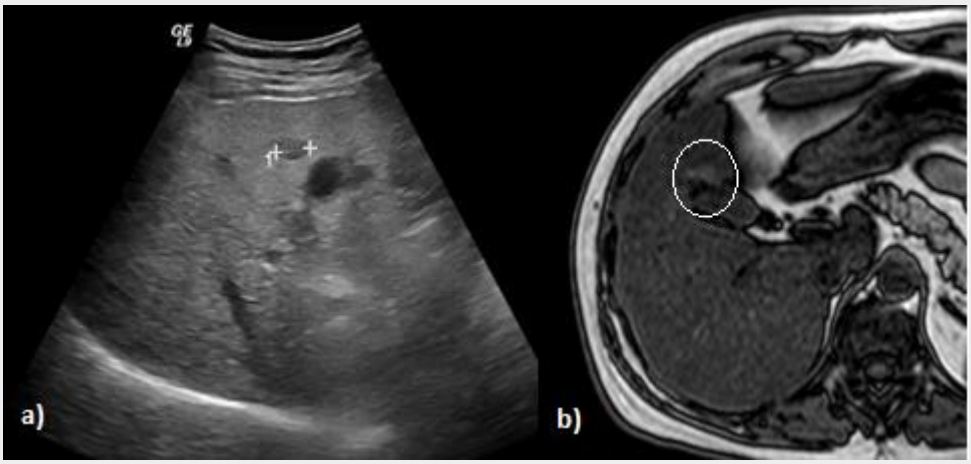

Figure 19 - Patient with a small hypo echogenic nodule near the gallbladder fossa in ultrasound study (a); also note the diffuse parenchyma increased ecogenicity. In MRI study no nodular lesion was found, except for a fat-sparing area near the gallbladder fossa seen in the T1-w out-of-phase imaging (b).

Perilesional fat sparing

This condition is not completely understood, but is thought to result from perfusion disturbances, either due to compression or invasion of portal venules by the tumor. Distribution can be peripheral, segmental or lobar (Figure 20).

Figure 20

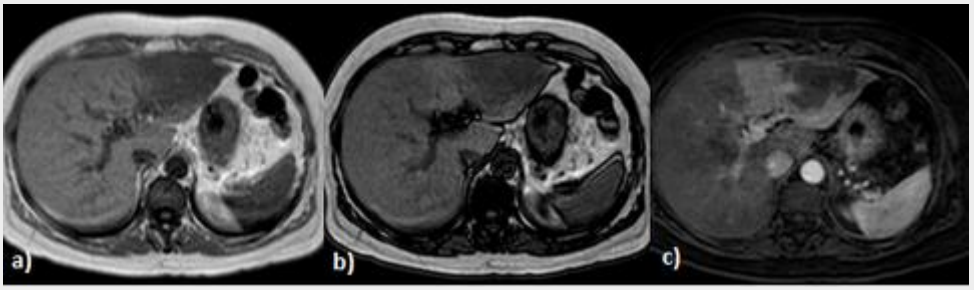

Figure 20 - Patient with an intrahepatic cholangiocarcinoma in the left lobe. In the MR T1-w out-of-phase imaging there is a more intense drop off of SI in the right lobe than the left lobe (a and b) revealing perilesional FFS. After gadolinium a more prominent arterial perfusion in the left lobe is visualized.

Some fatty changes can have an atypical distribution with a bizarre appearance (Figure 21).

Figure 21

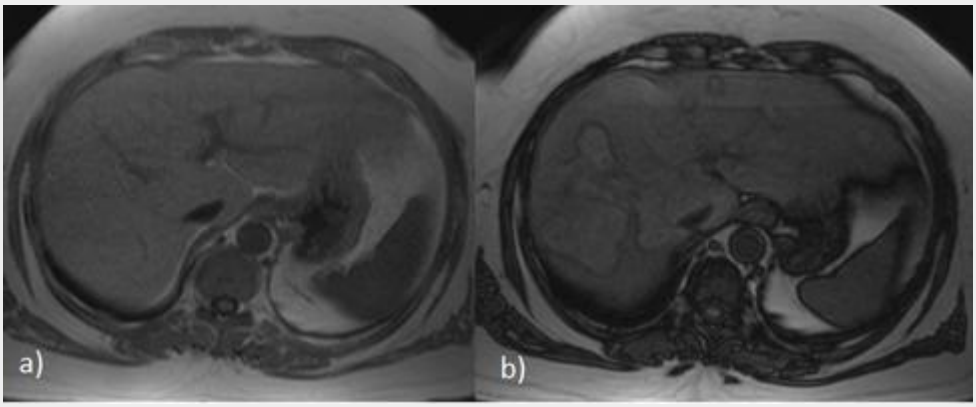

Figure 21 - MR T1-w in (a) and out-of-phase (b) imaging showing a bizarre fatty changes distribution, no other changes were found in other sequences.

Focal liver neoplasms with lipid content

Some primary liver neoplasms (e.g. hepatocellular adenoma, well-differentiated HCC and rare cases of FNH) can be more or less lipid-rich contributing to increase the diagnostic uncertainty.

Other rare hepatic lesions such as angiomyolipoma, lipoma, mielolipoma or metastatic lesions may also have a fat content

Hepatocellular carcinoma

Fat content in HCC is a histologically frequent finding but not easily identified in imaging studies. It's more frequent in smaller lesions; in large lesions a mosaic pattern may be found with areas of hemorrhage, fat and necrosis (Figures 22 and 23).

Figure 22

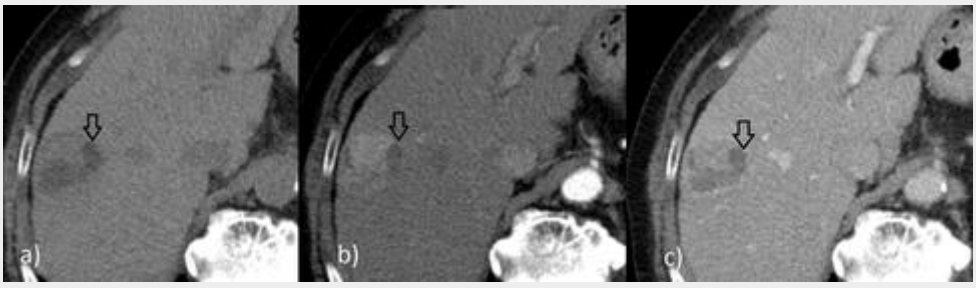

Figure 22 - CT axial images non-enhanced (a) and after contrast in arterial (b) and portal phase (c) in a patient with hepatocellular carcinoma. There are focal intralesional areas of lower attenuation (negative HU values) which don't enhance after contrast (black arrow) corresponding to fat. Other portions of the lesion are hypervascular (b) with washout in portal phase (c).

Figure 23

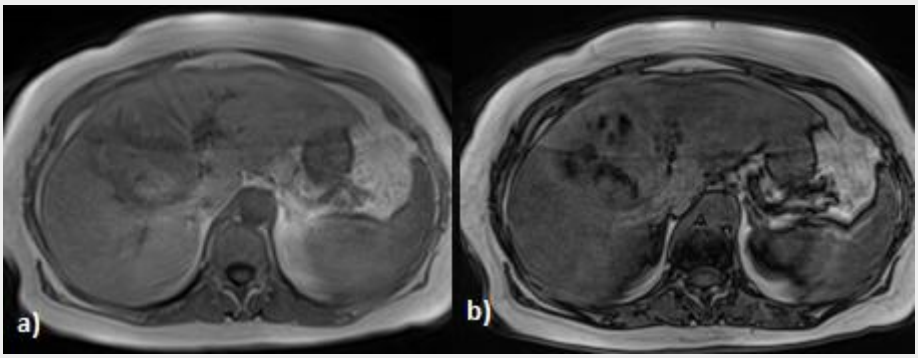

Figure 23 - MR T1-w in-phase (a) and out-of-phase imaging (b) in a patient with hepatocellular carcinoma. There are intralesional areas of significant drop-off of SI in out-of-phase imaging (b) due to the presence of intralesional fat.

Hepatocellular Adenoma

Adenoma occurs particularly in young and middle-aged women. Theses lesions have normal hepatocytes with no acinar structure. They are four major subtypes: (a) inflammatory/telangiectatic, (b) steatotic with HNF-1α gene mutation, (c) with β-catenin activation (d) and an additional unclassified/miscellaneous subgroup. Steatotic subtype is about 35%-50% of hepatocellular adenomas. It has no risk of malignant transformation. Familial adenomatosis and MODY-3 diabetes mellitus may be associated. It occurs due to lack of expression of liver fatty acid binding protein (LFABP) (Figure 24).

Figure 24

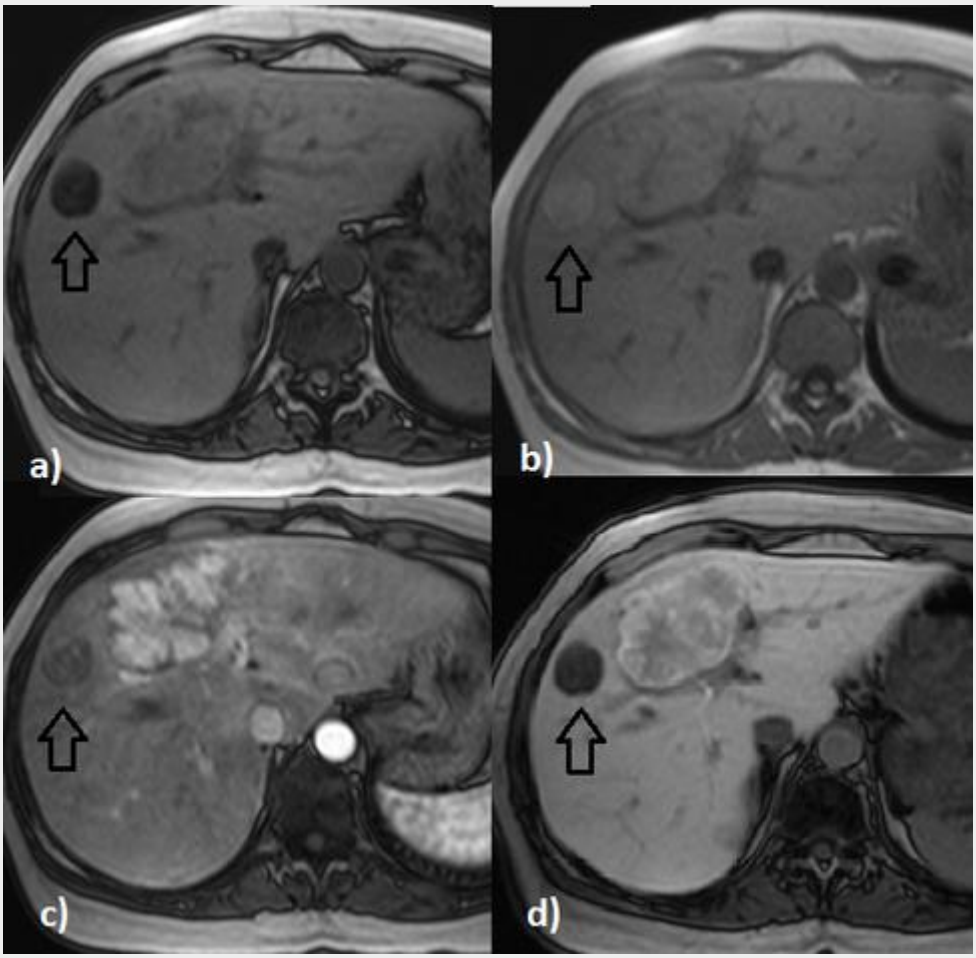

Figure 24 - Steatotic hepatocellular adenoma. There is a sharply-marginated nodule (black arrow) hypointense in T1-w out-of-phase (a) sequence and hyperintense on T1-w in-phase image (b), findings indicative of fatty metamorphosis. It shows only mild enhancement on the dynamic study performed with Gd-BOPTA, particularly during the arterial phase (c), appearing hypointense on the delayed image (d). Note a large-sized FNH near to it.

Adenomatosis (10 or more adenomas) may be difficult to differentiate from multifocal nodular steatosis, but no enhancement is seen in the latest.

Focal Nodular Hyperplasia

Fat content is very rare in Focal Nodular Hyperplasia (FNH), but it can occur, if a typical presentation is found (hypervascular with central scar) diagnosis can be made, nevertheless biopsy may be required in some cases. Well differentiated hepatocellular carcinoma is the most important differential diagnosis (Figure 25).

Figure 25

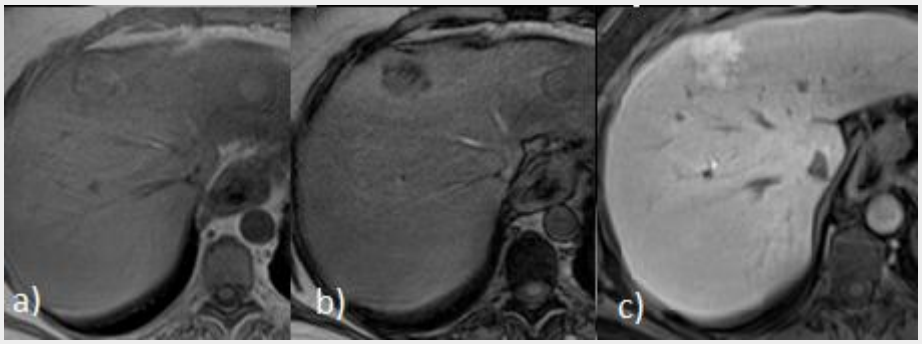

Figure 25 - MR T1-w in and out-of-phase imaging (a and b) showing the presence of intralesional fat (SI drop-off). After hepatospecific contrast, there is contrast retention in the hepatobiliary phase (c), a characteristic feature of FNH but that can also occur in well differentiated hepatocellular carcinoma.

Other lesions

Some fat containing hepatic lesions are very rare.

Hepatic lipoma is generally asymptomatic. It appears as an homogenous mass with regular borders and no enhancement after contrast. Attenuation/SI is equal to subcutaneous fat (Figures 26 and 27).

Figure 26

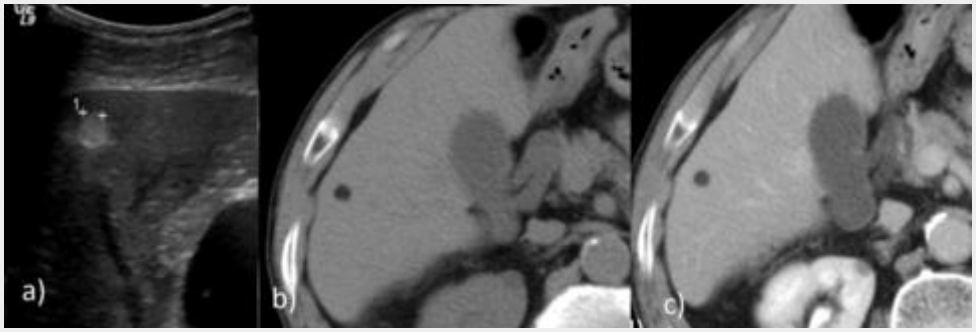

Figure 26 -Patient with a small hepatic lipoma. In ultrasound there is a hyper echogenic small lesion (a), that has a very low attenuation in CT study equal to subcutaneous fat (b), no enhancement was found after contrast injection (c).

Figure 27

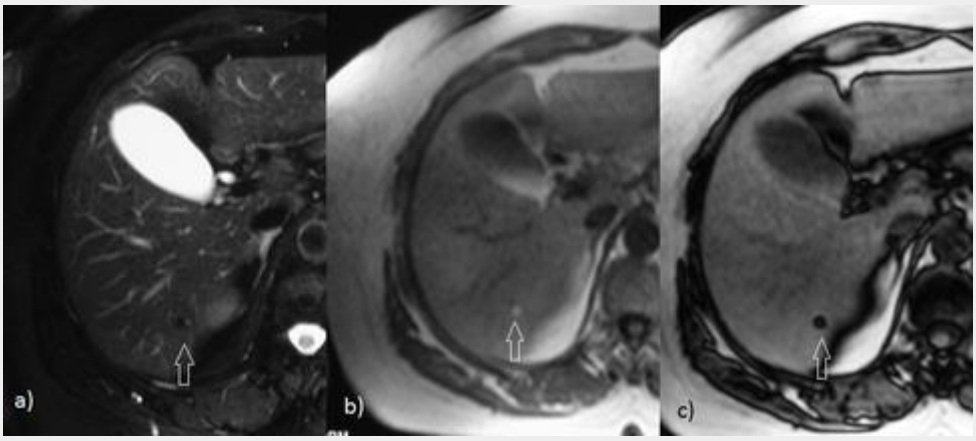

Figure 27 - Hepatic lipoma. MRI study showing a tiny nodule on the right liver lobe with low SI on the T2-w FS sequence (a) and hyperintense on the in-phase T1-w image (b); the indian ink artifact around the lesion due to susceptibility artifact in the boundary between the tumor fat and the adjacent liver parenchyma on the out-of-phase image (c) almost obscures it.

Angiomyolipoma is associated with certain syndromes (e.g. tuberous sclerosis). Three patterns based in the grade of soft tissues and fat content are described (Figure 28).

Figure 28

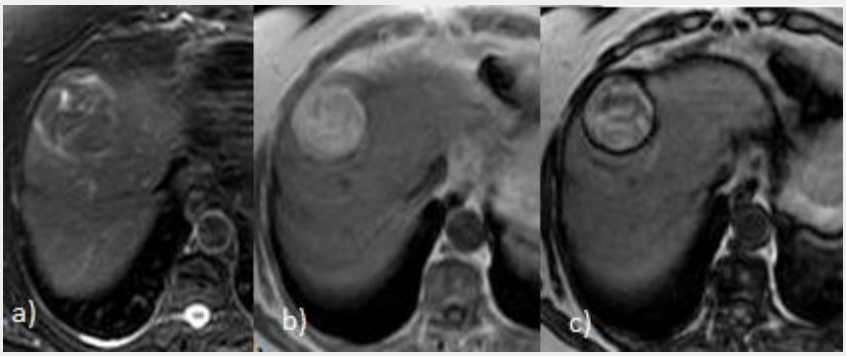

Figure 28 - Hepatic angiomyolipoma: the lesion appears dark on the T2-w FS image (a), and as bright as the sub-cutaneous fat on the in-phase T1-w sequence (b); note the indian ink artifact around the lesion on the out-of-phase image (c), due to chemical shift artifact in the boundary between fat within the tumor and the adjacent liver parenchyma.

Metastatic disease is extremely rare, but described in some tumors: ovarian dermoids, teratomas, liposarcoma, Wilm's tumor and renal cell carcinoma.

4. Conclusion

Cross-sectional Imaging techniques allow a non-invasive diagnosis of focal forms of liver steatosis and fat sparing, differentiating pseudo-nodular presentations from true liver tumors.

Although US and CT allow the potential evaluation of those patients, MR is superior due to its intrinsic contrast resolution and functional information capabilities.

5. References

Carlos Valls, Ricardo Iannacconne, Esther Alba, Takamichi Murakami, Masatoshi Hori, Roberto Passariello, Valérie Vilgrain. Fat in the liver: diagnosis and characterization, European Radiology October 2006, Volume 16, Issue 10, pp 2292-2308

Desser TS., Understanding transient hepatic attenuation differences. Semin Ultrasound CT MR. 2009 Oct;30(5):408-17.

Gourtsoyiannis NC. Clinical MRI of the AbdomenWhy,How,When. Springer 2011

Leitao H S, Paulino C, Rodrigues D, Goncalves S, Marques C, Carvalheiro M et al. MR Fat Fraction Mapping: A Simple Biomarker for Liver Steatosis Quantification in Nonalcoholic Fatty Liver Disease Patients, Acad Radiol 2013; 20:957–961

Wanless IR, Bargman JM, Oreopoulos DG, Vas SI. Subcapsular steatonecrosis in response to peritoneal insulin delivery: a clue to the pathogenesis of steatonecrosis in obesity.Mod Pathol 1989;2:69–74

6. Author Information

Catarina Oliveira, kat.catarina@gmail.com

7. Mediafiles

Figure 1

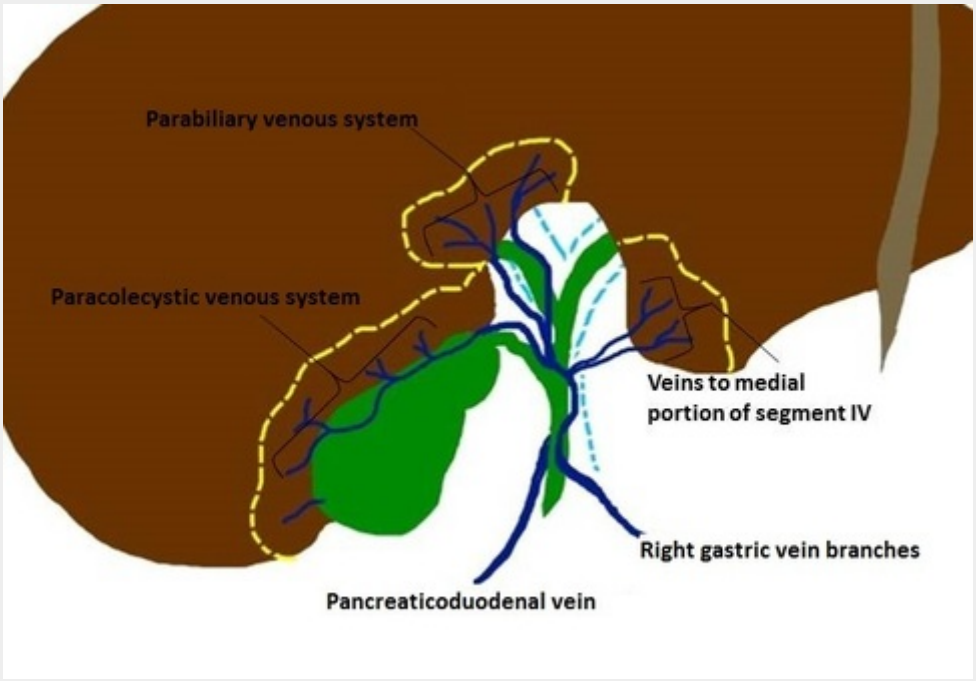

Figure 1 - Schematic draw showing parabiliary and paracolecystic venous system and branches from pancreaticoduodenal and right gastric veins responsible for anomalous venous flow in characteristic parenchymal areas.

Figure 2

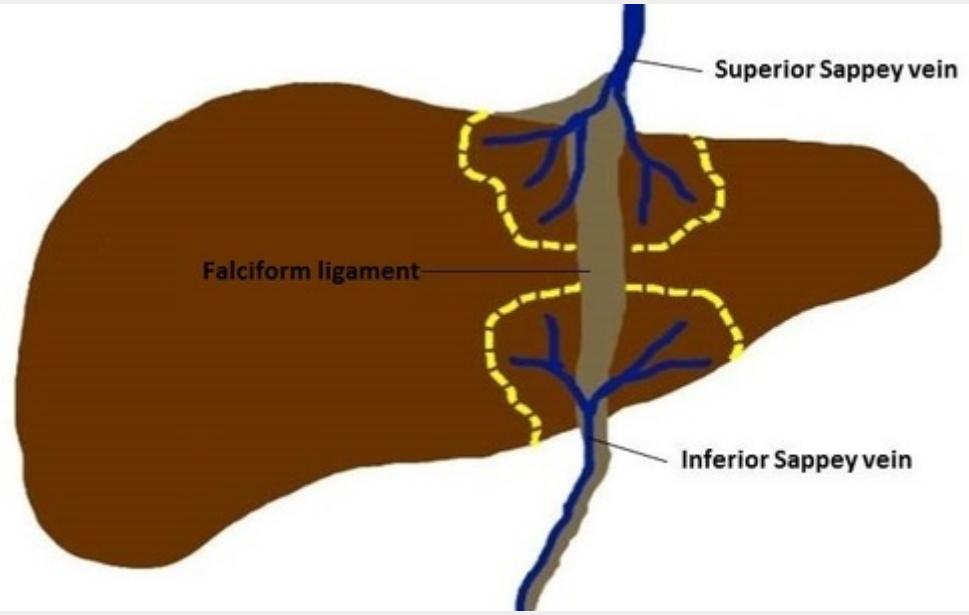

Figure 2 - Schematic draw showing superior and inferior Sappey veins responsible for anomalous venous flow near the falciform ligament.

Figure 3

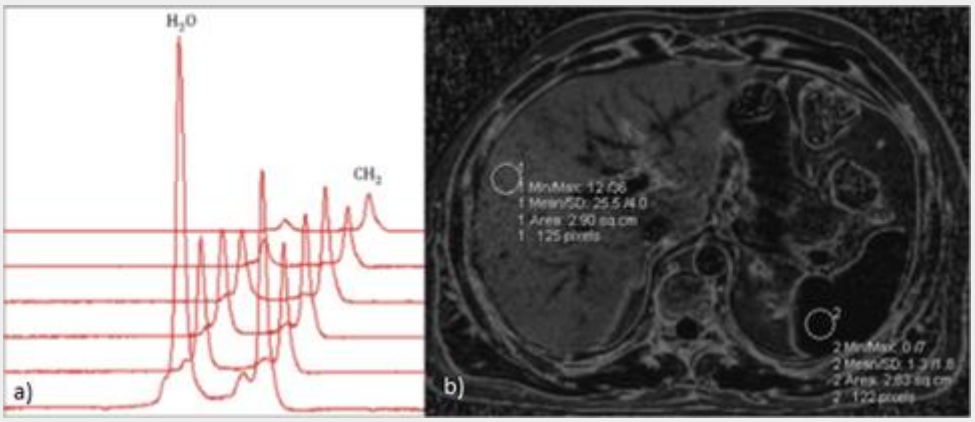

Figure 3 - Patient with hepatic steatosis. MRS analyses (a) and fat fraction mapping analyse (b) in a fat quantification study.

Figure 4

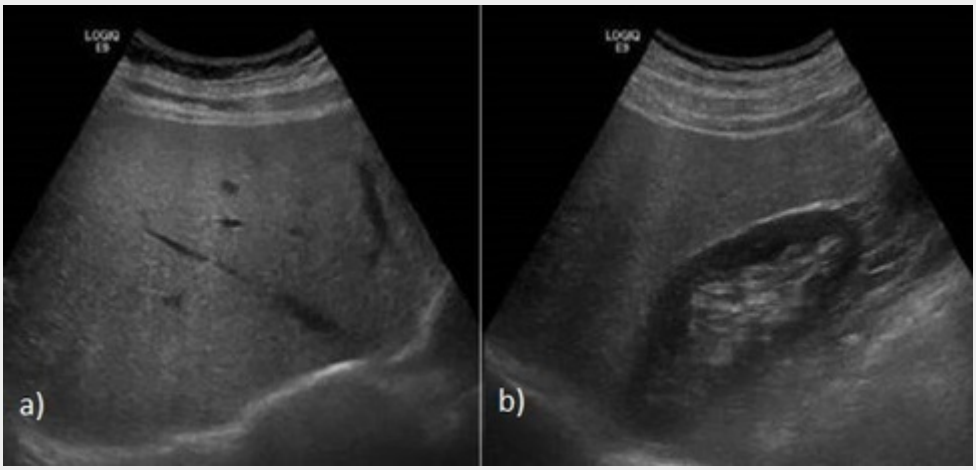

Figure 4 - Ultrasound images in a patient with diffuse hepatic steatosis showing increased hepatic parenchyma echogenicity (a). Note the reflectivity differences between the liver and the right kidney (b).

Figure 5

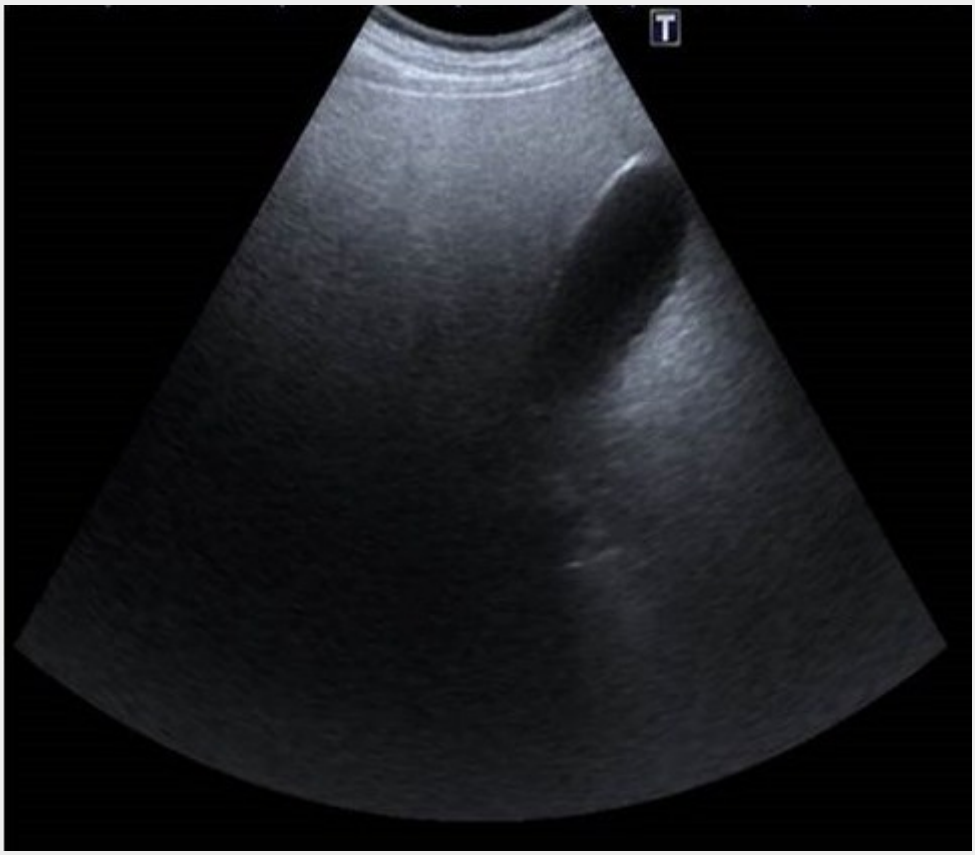

Figure 5 - Ultrasound image in a severe case of hepatic steatosis. There is a very high attenuation of the ultrasound beam caused by the diffuse fat infiltration.

Figure 6

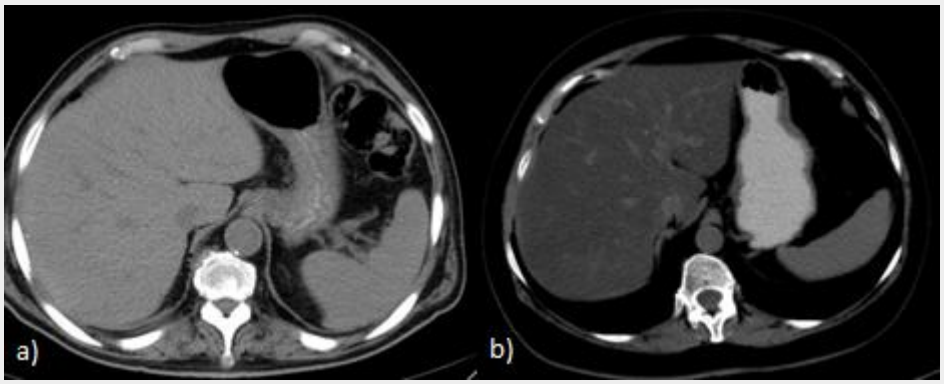

Figure 6 - CT non-contrast axial images showing normal hepatic parenchyma density (a) and a severe case of diffuse fat infiltration with a reversed vascular pattern (b).

Figure 7

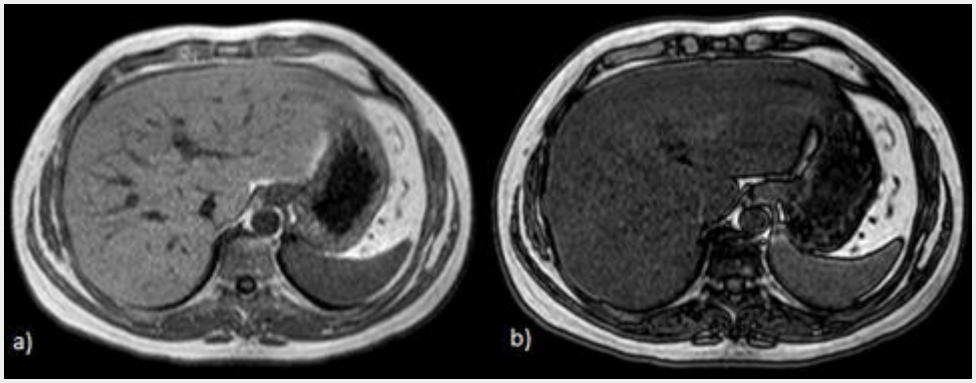

Figure 7 - MR T1-w in-phase (a) and out-of-phase imaging (b). Note the diffuse drop-off of SI in out-of-phase imaging (b) due to the presence of microscopic fat.

Figure 8

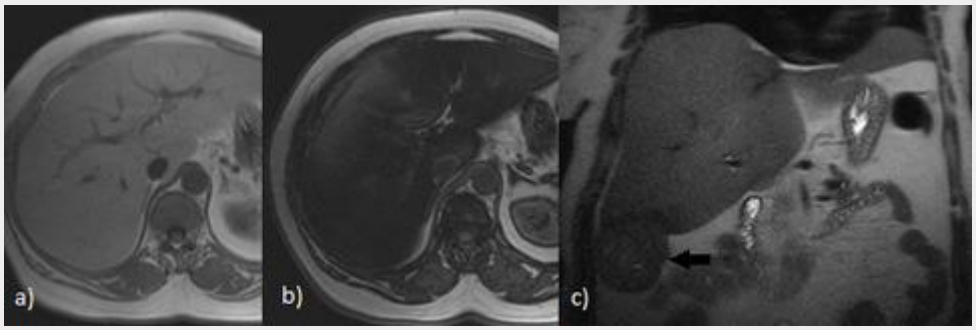

Figure 8 - MR T1-w in-phase (a) and out-of-phase imaging (b) showing diffuse hepatic steatosis. (c) MR T2-w imaging in the coronal plane of the same patient revealing a nodular lesion (black arrow): a hepatocellular carcinoma diagnosis was made.

Figure 9

Figure 9 - Ultrasound image showing a nodular periportal hyperechogenic lesion in a midle-age female patient.

Figure 10

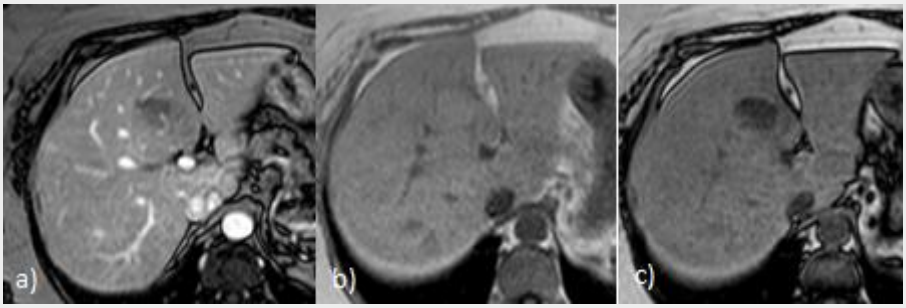

Figure 10 - Same patient in Figure 9. MR axial T1-w imaging after gadolinium injection (a) no vessel distortion is noted. In T1-w in-phase (b) and out-of-phase (c) imaging there is a diffuse SI drop-off in out-of-phase sequence confirming that the nodular area corresponds to a focal fat infiltration area.

Figure 11

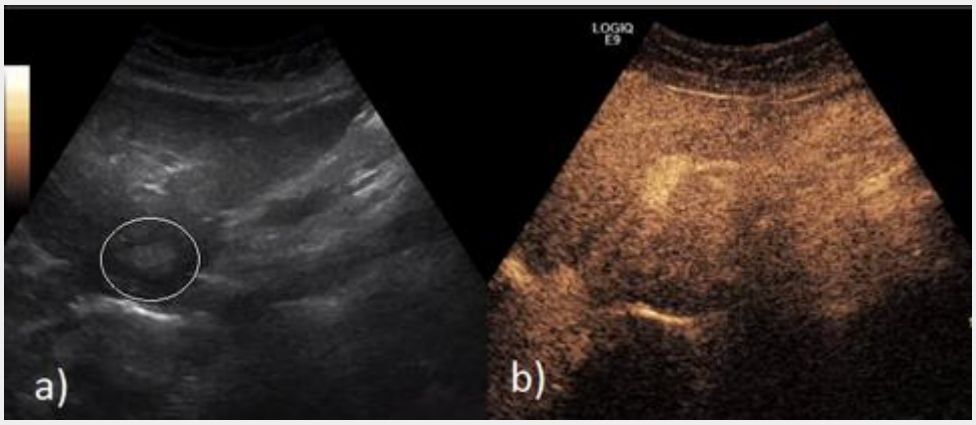

Figure 11 - Contrast enhanced US may help to identified focal fat infiltration areas. In steatotic areas, enhancement equals the rest of the liver parenchyma (b); fat infiltration area is only identified in B-mode images (a).

Figure 12

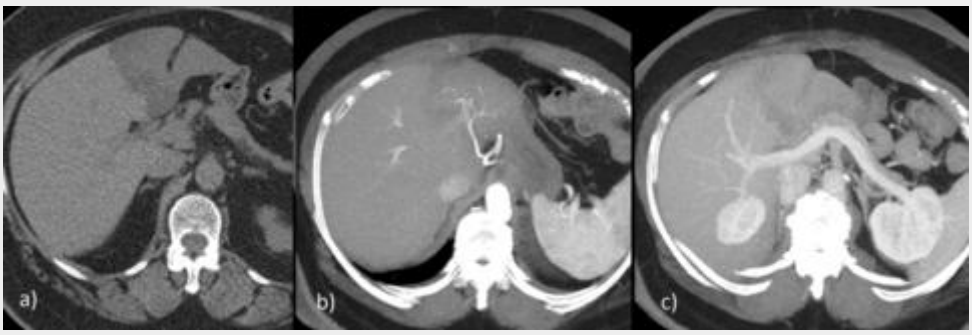

Figure 12 - CT axial image (a) and MIP reconstructions (b and c) showing a segmental fat infiltration distribution. In non-enhanced image there is diffuse low attenuation in the left lobe (a), post contrast in late arterial (b) and portal phase (c) reveal an increase in arterial flow by left gastric artery branches (b) and no left portal venous flow (c).

Figure 13

Figure 13 - Subcapsular steatosis. Non-enhanced CT images (a to c) in a patient with a subcapsular distribution of fat infiltration (lower attenuation areas).

Figure 14

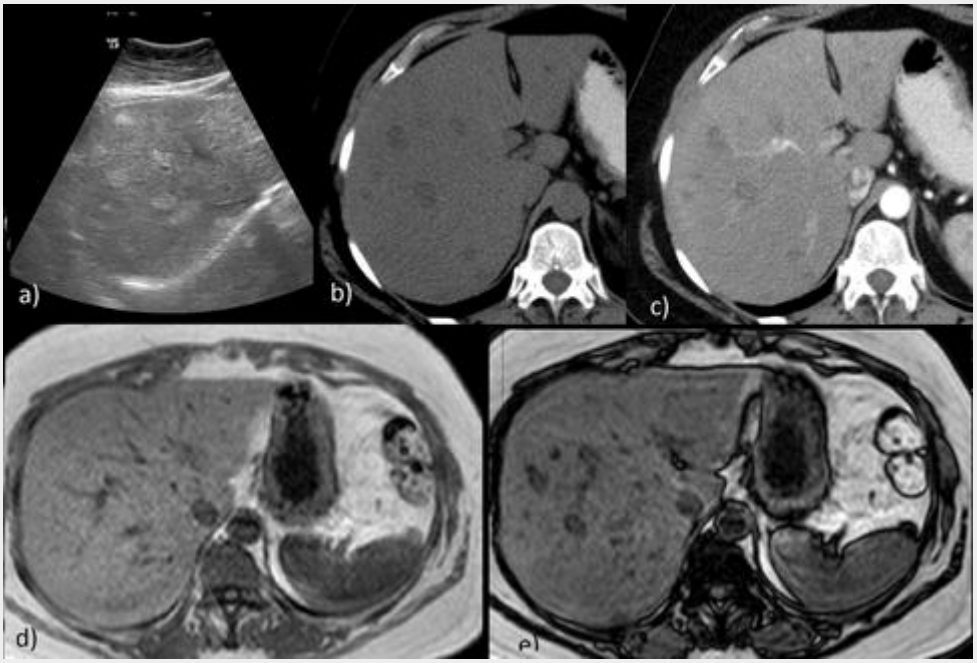

Figure 14 - Multinodular steatosis. Ultrasound (a) shows hyper echogenic nodular lesions; in CT axial non-enhanced images there are several hypo attenuated lesions that don't enhance after contrast (b and c). In MRI T1-w out-of-phase imaging there is SI drop-off of the nodular lesions (e).

Figure 15

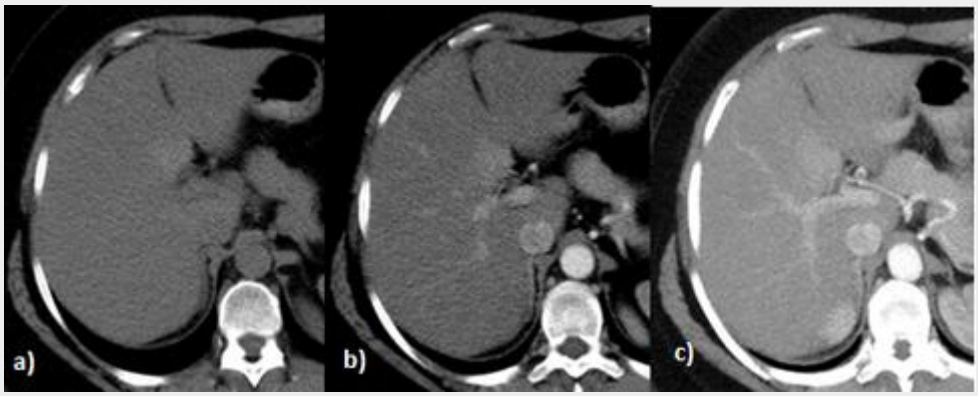

Figure 15 - Focal fat sparing in the postero medial portion of IV hepatic segment. There is a discrete higher attenuation in non-enhanced image (a). After contrast we can see that there is no vascular distortion (a vessel runs through it) and the geographical margins are better defined (b and c).

Figure 16

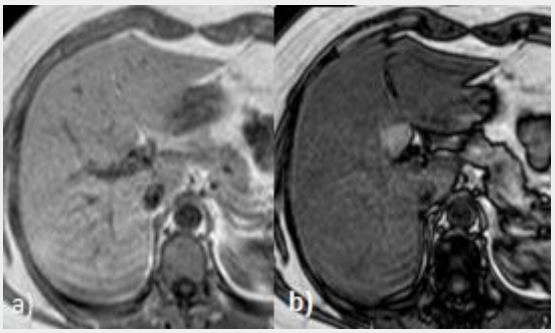

Figure 16 - Same patient in Figure 13. In MR T1-w out-of-phase imaging (b) there is a diffuse drop-out of SI, except in the posterior medial aspect of the IV segment - focal fat sparing.

Figure 17

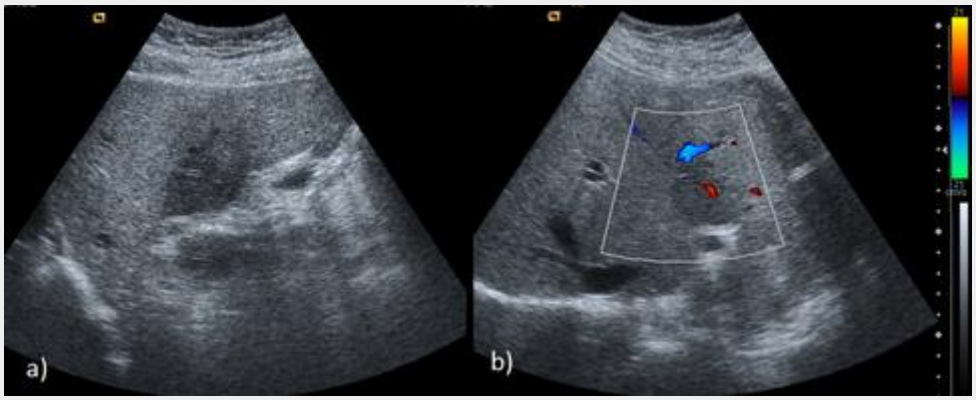

Figure 17 - Ultrasound images showing a hypoechoic area in the left lobe (a); no vessel distortion is shown in Doppler study (b); these are characteristic features of FFS area. No enhancing lesion was found in CT study (not shown).

Figure 18

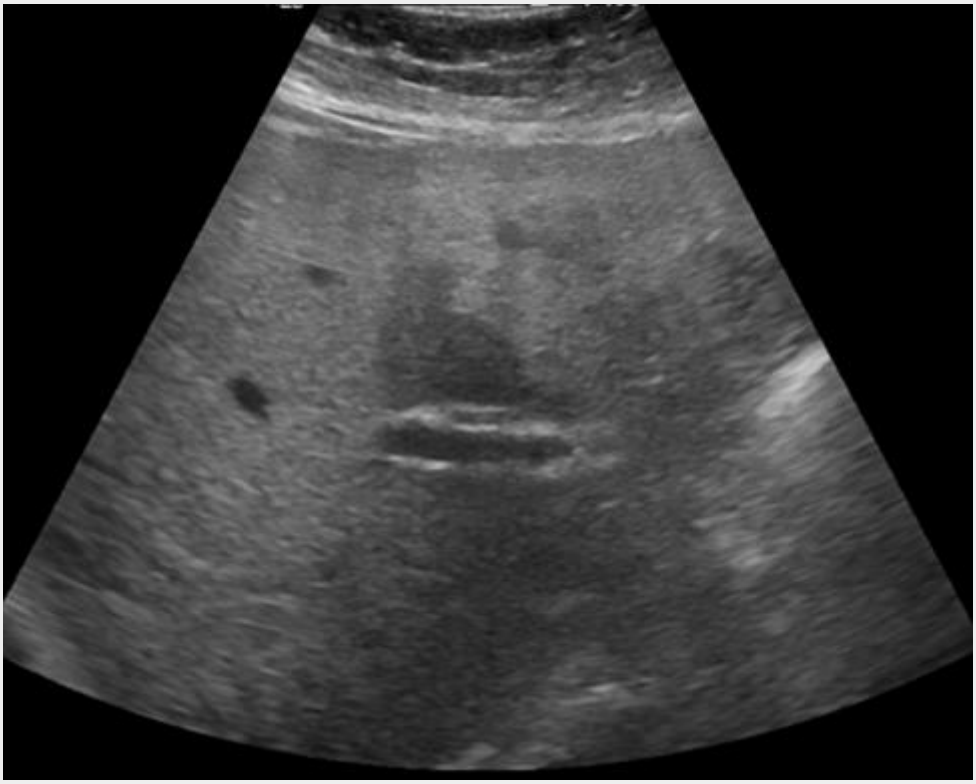

Figure 18 - Typical periportal location of FFS. Note the geographical margins and no mass-effect of the hypoechoic area.

Figure 19

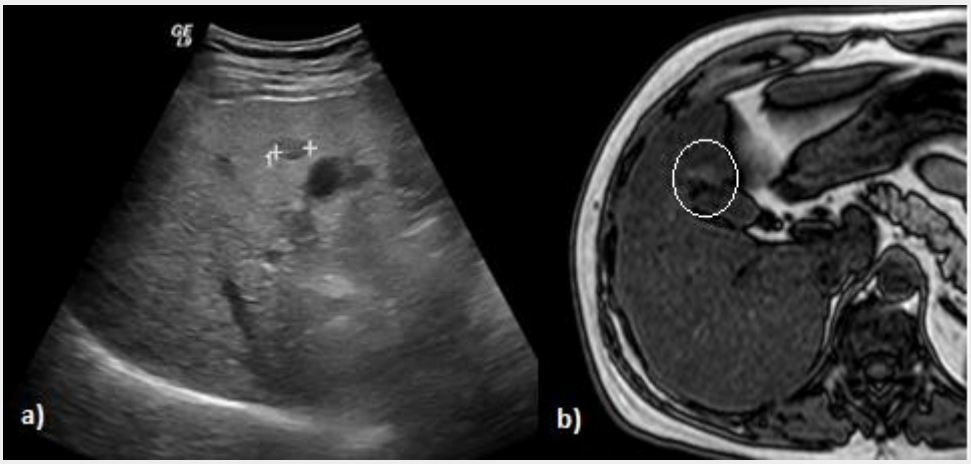

Figure 19 - Patient with a small hypo echogenic nodule near the gallbladder fossa in ultrasound study (a); also note the diffuse parenchyma increased ecogenicity. In MRI study no nodular lesion was found, except for a fat-sparing area near the gallbladder fossa seen in the T1-w out-of-phase imaging (b).

Figure 20

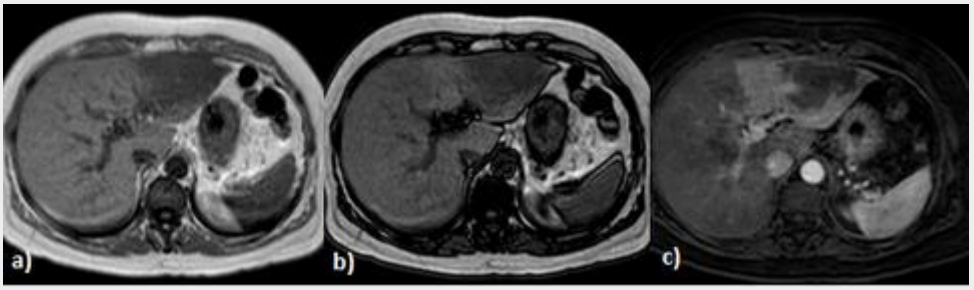

Figure 20 - Patient with an intrahepatic cholangiocarcinoma in the left lobe. In the MR T1-w out-of-phase imaging there is a more intense drop off of SI in the right lobe than the left lobe (a and b) revealing perilesional FFS. After gadolinium a more prominent arterial perfusion in the left lobe is visualized.

Figure 21

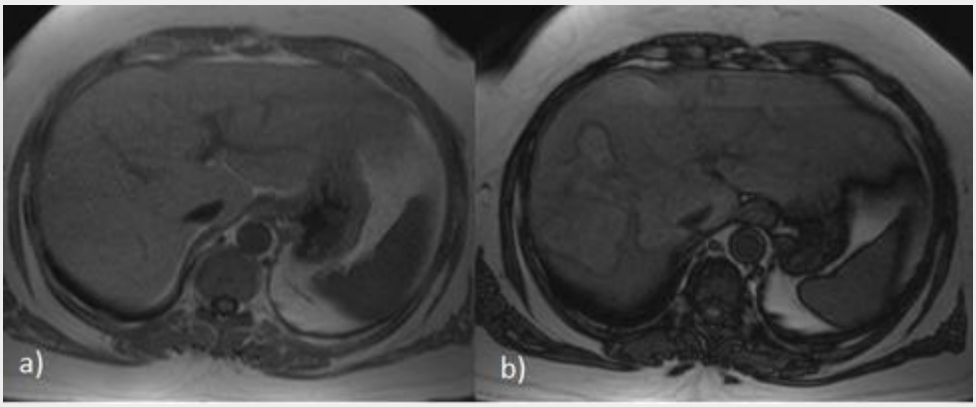

Figure 21 - MR T1-w in (a) and out-of-phase (b) imaging showing a bizarre fatty changes distribution, no other changes were found in other sequences.

Figure 22

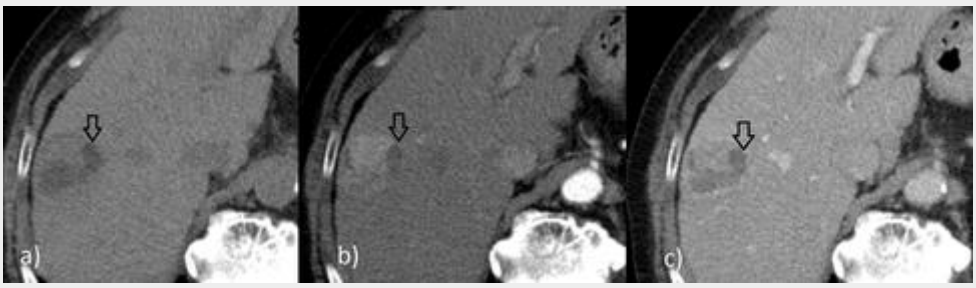

Figure 22 - CT axial images non-enhanced (a) and after contrast in arterial (b) and portal phase (c) in a patient with hepatocellular carcinoma. There are focal intralesional areas of lower attenuation (negative HU values) which don't enhance after contrast (black arrow) corresponding to fat. Other portions of the lesion are hypervascular (b) with washout in portal phase (c).

Figure 23

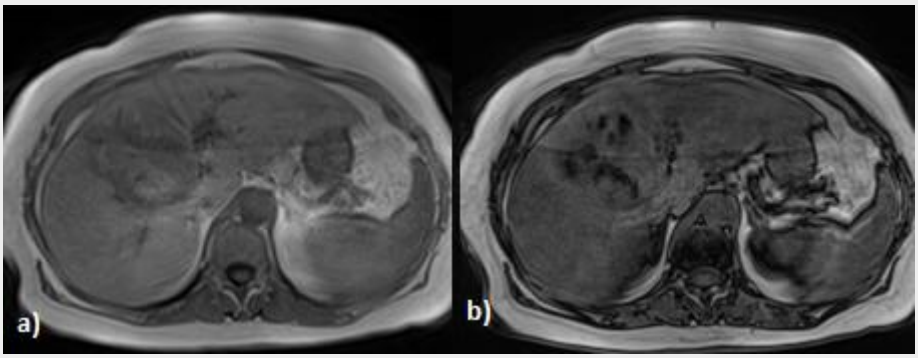

Figure 23 - MR T1-w in-phase (a) and out-of-phase imaging (b) in a patient with hepatocellular carcinoma. There are intralesional areas of significant drop-off of SI in out-of-phase imaging (b) due to the presence of intralesional fat.

Figure 24

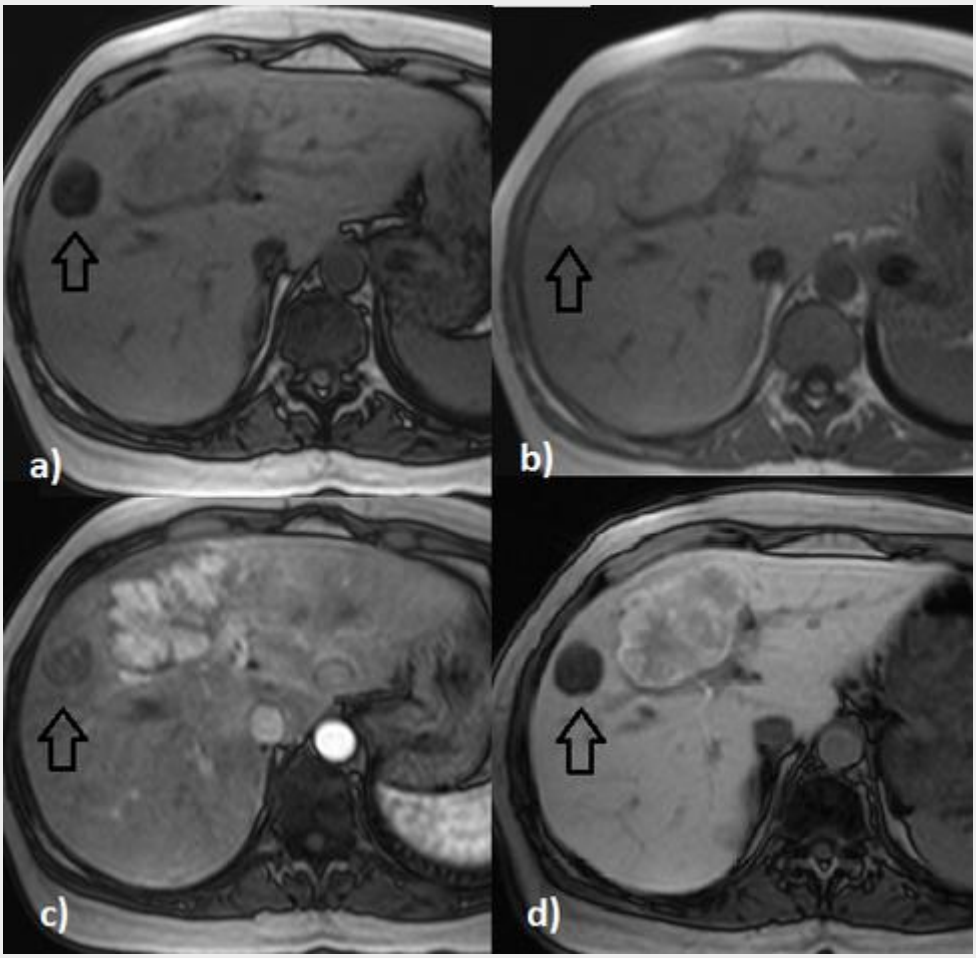

Figure 24 - Steatotic hepatocellular adenoma. There is a sharply-marginated nodule (black arrow) hypointense in T1-w out-of-phase (a) sequence and hyperintense on T1-w in-phase image (b), findings indicative of fatty metamorphosis. It shows only mild enhancement on the dynamic study performed with Gd-BOPTA , particularly during the arterial phase (c), appearing hypointense on the delayed image (d). Note a large-sized FNH near to it.

Figure 25

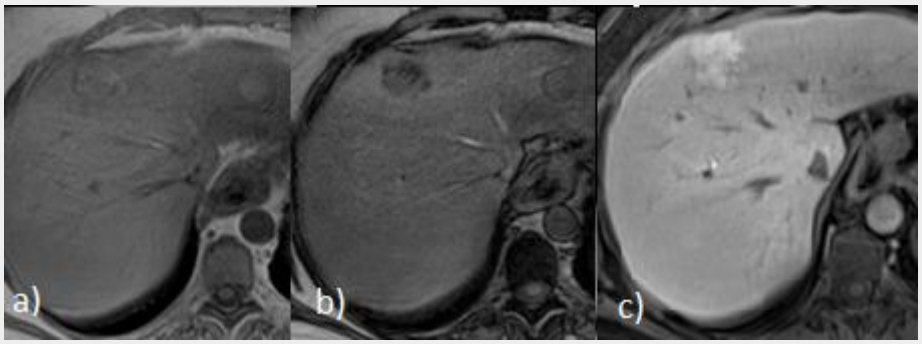

Figure 25 - MR T1-w in and out-of-phase imaging (a and b) showing the presence of intralesional fat (SI drop-off). After hepatospecific contrast, there is contrast retention in the hepatobiliary phase (c), a characteristic feature of FNH but that can also occur in well differentiated hepatocellular carcinoma.

Figure 26

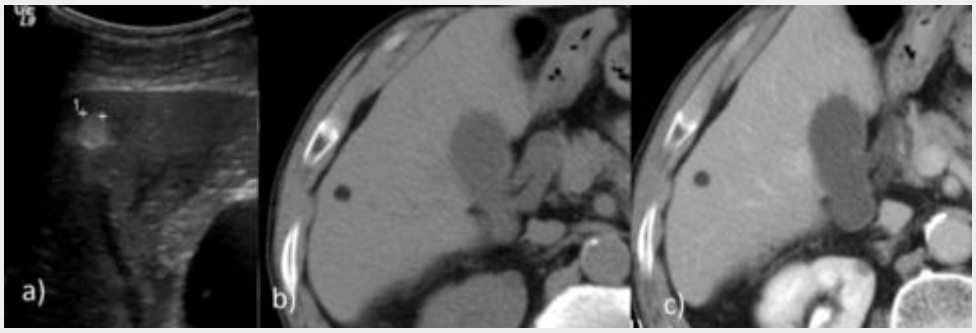

Figure 26 -Patient with a small hepatic lipoma. In ultrasound there is a hyper echogenic small lesion (a), that has a very low attenuation in CT study equal to subcutaneous fat (b), no enhancement was found after contrast injection (c).

Figure 27

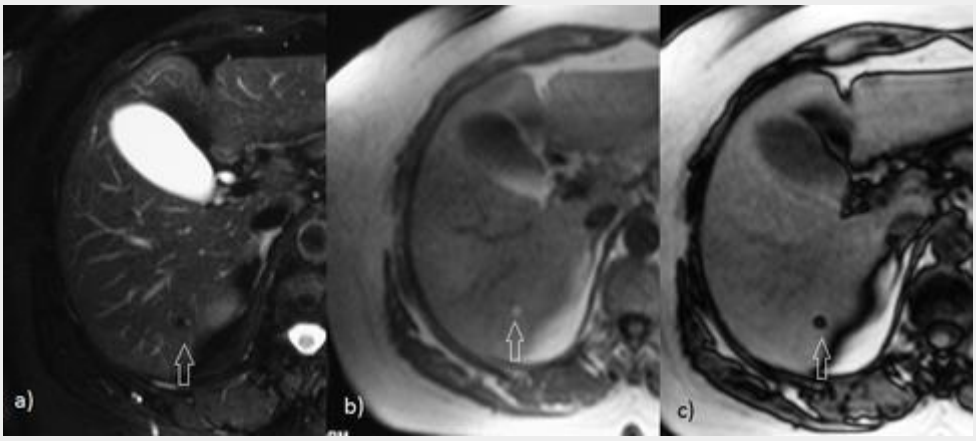

Figure 27 - Hepatic lipoma. MRI study showing a tiny nodule on the right liver lobe with low SI on the T2-w FS sequence (a) and hyperintense on the in-phase T1-w image (b); the indian ink artifact around the lesion due to susceptibility artifact in the boundary between the tumor fat and the adjacent liver parenchyma on the out-of-phase image (c) almost obscures it.

Figure 28

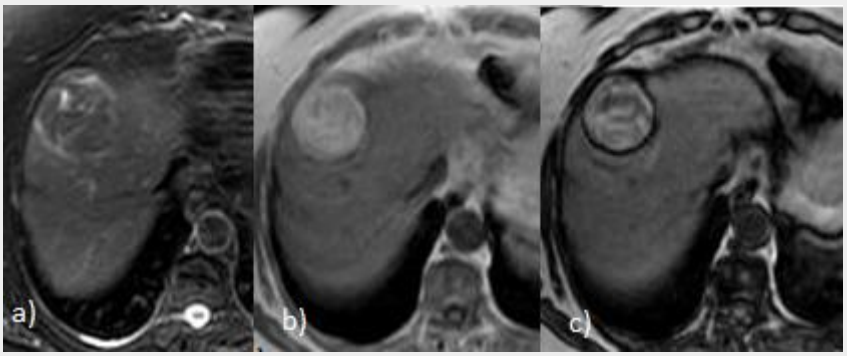

Figure 28 - Hepatic angiomyolipoma: the lesion appears dark on the T2-w FS image (a), and as bright as the sub-cutaneous fat on the in-phase T1-w sequence (b); note the indian ink artifact around the lesion on the out-of-phase image (c), due to chemical shift artifact in the boundary between fat within the tumor and the adjacent liver parenchyma.

Table 1

	Pattern distribution
Steatosis	Diffuse Focal - Nodular - Subcapsular - Perivascular - Perilesional Multinodular
Fat sparing	Focal - Nodular - Subcapsular - Perivascular - Perilesional

Table 1 - Pattern distribution types of steatosis and fat sparing in the liver.

Table 2

Location	Abnormal venous flow
Medial portion of segment IV	Gastric or pancreaticoduodenal veins
Adjacent to the *porta hepatis*	Parabiliary venous system
Adjacent to the falciform ligament	Sappey veins
Gallbladder fossa	Paracolecystic venous system
Subcapsular parenchyma	Subfrenic veins

Table 2 - Typical locations of focal fat changes in hepatic parenchyma.